

## An MPDATA-based solver for compressible flows

Piotr K. Smolarkiewicz<sup>1</sup> and Joanna Szmelter<sup>2,\*</sup>,<sup>†</sup>

<sup>1</sup>*National Center for Atmospheric Research, Boulder, CO 80307, U.S.A.*

<sup>2</sup>*Loughborough University, Leicestershire LE11 3TU, U.K.*

### SUMMARY

The theory of the high-resolution multidimensional positive-definite advection transport algorithm (MPDATA) has been extensively developed since its invention in the early eighties. Many successful applications for geophysical flows followed. This paper introduces the original development of an MPDATA solver operating on a classical set of conservation laws, applicable to high-speed compressible flows. The solver belongs to a general class of the second-order nonoscillatory forward-in-time schemes. Theoretical considerations are supported with numerical examples. An elementary three-dimensional spherical wave-propagation problem illustrates that MPDATA correctly captures signal transfer in acoustic flows. Copyright © 2007 John Wiley & Sons, Ltd.

Received 30 March 2007; Revised 28 August 2007; Accepted 30 August 2007

KEY WORDS: nonoscillatory forward-in-time schemes; compressible flows; upwind approximations

### 1. THEORETICAL CONSIDERATIONS

An abstract theory of nonoscillatory forward-in-time (NFT) methods for fluids<sup>‡</sup> has been put forward in the early nineties [1, 2]. In principle, NFT solvers can operate on various forms of fluid equations—see [3] in the same issue, for a discussion of anelastic systems—and they can be implemented using any nonlinearly stable (e.g. nonoscillatory) two-time-level advection (convection) algorithm that is at least second-order accurate for an arbitrary time-independent flow. Our method of choice is MPDATA [4–6] for its genuine multidimensionality, easy accuracy-sustaining generalization to unstructured meshes [7], and suitability for direct numerical simulation (DNS), large eddy simulation (LES), and implicit large eddy simulation (ILES) [8].

---

\*Correspondence to: Joanna Szmelter, Loughborough University, Leicestershire LE11 3TU, U.K.

<sup>†</sup>E-mail: j.szmelter@lboro.ac.uk

<sup>‡</sup>The term ‘nonoscillatory forward-in-time’ labels a class of second-order-accurate two-time-level algorithms built on nonlinear advection techniques that suppress/reduce/control numerical oscillations characteristic of higher-order linear schemes; and is meant to distinguish these algorithms from classical centered-in-time-and-space linear methods, but not to imply perfectly oscillation-free solutions.

The underlying theory of NFT solvers derives from the truncation-error analysis of upwind approximations for an archetype inhomogeneous partial differential equation (PDE) for fluids

$$\frac{\partial \phi}{\partial t} + \nabla \cdot (\mathbf{V}\phi) = R \quad (1)$$

in abstraction from any particular assumptions on the nature of physical forcings  $R$ , and their relation to dependent-variable densities  $\phi$ , but driven solely by the requirement of the second-order accuracy for an arbitrary velocity field  $\mathbf{V}(\mathbf{x}, t)$ . One resulting template algorithm for (1) takes a particularly simple and compact form

$$\phi_i^{n+1} = \mathcal{A}_i(\phi^n + 0.5\delta t R^n, \mathbf{V}^{n+1/2}) + 0.5\delta t R^{n+1} \quad (2)$$

Here  $n$  and  $i$  refer to the temporal and spatial position on the mesh,  $\mathcal{A}$  symbolizes a two-time level nonoscillatory transport operator (viz. advection scheme) assumed second-order accurate for a homogeneous case of (1) with time-independent  $\mathbf{V}$ . Furthermore,  $\mathbf{V}^{n+1/2}$  is an  $\mathcal{O}(\delta t^2)$  estimate of  $\mathbf{V}$  at  $t + 0.5\delta t$ , and  $R^{n+1} = R(t + \delta t) + \mathcal{O}(\delta t^3)$  can either be an explicit estimate or depend implicitly on all relevant problem variables  $\phi$ .

In (2) there are two key elements defining the solver: (i) the choice of the transport operator  $\mathcal{A}$ ; and (ii) the approach for evaluating  $R^{n+1}$  on the rhs. The latter depends on the adopted form of the conservation laws and selection of dependent variables. In contrast to the proven record in computing incompressible and anelastic flows [8], there is little experience with the NFT simulations of gas dynamics. Except for its simplest isentropic limit [7, 9]—convenient to illustrate the mechanics of MPDATA-based NFT methods—the efficacy of the NFT solvers for compressible flows is largely unknown.

Herein, we extend the previous work [7, 9] to solve the standard set of conservation laws used in the simulation of gas dynamics. The Euler equations for mass, momentum, and total energy are expressed in the form adhering to (1), respectively, as:

$$\frac{\partial \rho}{\partial t} + \nabla \cdot (\mathbf{V}\rho) = 0 \quad (3)$$

where  $\rho$  denotes gas density;

$$\frac{\partial q^I}{\partial t} + \nabla \cdot (\mathbf{V}q^I) = -\frac{\partial p}{\partial x^I} \quad (4)$$

where  $q^I \equiv \rho V^I$  (for  $I = 1, 2, 3$ ) denote momenta and  $p$  stands for pressure; and

$$\frac{\partial E}{\partial t} + \nabla \cdot (\mathbf{V}E) = -\nabla \cdot (\mathbf{V}p) \quad (5)$$

with  $E \equiv \rho e + (1/2)\rho \mathbf{V}^2$ , wherein  $e = c_v T$  is the specific internal energy, while  $T$  and  $c_v$  denote the temperature and specific heat at constant volume.

In general, solving (4) and (5) implies an implicit problem due to the dependence of pressure on the energy and flow. We proceed in the spirit of the Crank–Nicholson schemes, by iterating (2)

$$\phi_i^{n+1, \mu} = \mathcal{A}_i(\phi^n + 0.5\delta t R^n, \mathbf{V}^{n+1/2}) + 0.5\delta t R^{n+1, \mu-1} \equiv \phi_i^* + 0.5\delta t R_i^{n+1, \mu-1} \quad (6)$$

where  $\mu = 1, \dots, m$  numbers successive iterations, and the first guess  $R^{n+1, 0}$  is either a first-order predictor or, simply,  $R^{n+1, 0} = R^n$ . Importantly, the computationally intensive explicit part  $\phi_i^*$  is

evaluated only once per time step—by executing an advection module prior to (6)—thus remaining fixed during the iteration process. Using  $\delta t$  that satisfies the Courant–Friedrichs–Lewy stability condition for the integrated PDE system (1) suffices for a rapid convergence of (6)—even with  $R^{n+1,0} = R^n$ ,  $m=2$  provides second-order-accurate solutions to (1), while  $m=3$  also ensures an  $\mathcal{O}(\delta t^3)$  estimate of  $R^{n+1}$  proven advantageous for the accuracy of NFT schemes [2].

## 2. RESULTS

### 2.1. Spherical acoustic wave

Statements appear in the literature implying that upwind approximations are inadequate for simulating propagation of acoustic modes. While this may be true for some upwind schemes, one should withhold generalizations as upwinding may take different forms and operate on a variety of auxiliary-dependent variables. In particular, MPDATA is constructed using properties of iterated upwinding, yet when applied in accord with the notion of NFT methods, it is capable of simulating difficult problems of wave dynamics. For substantiation, we paraphrase the classical problem of a spherical sound wave propagation (Problem 1 in Section 70, Chapter VIII of [10]). The problem considers ‘a sound wave in which the distribution of density, velocity, and other flow variables, depends only on the distance from some point’. It employs the spherical wave equation for the velocity potential in the zero free-stream Mach number limit. Assuming initial sphere of radius  $r_0$  compressed so that density excess  $\rho' = \delta\rho = \text{const}$  for  $r \leq r_0$  and  $\rho' \equiv 0$  otherwise, it evinces the analytic solution (away from the initial disturbance region) in the form of the spherical shell of thickness  $2r_0$ , located at  $r \in [c_0 t - r_0, c_0 t + r_0]$ , where  $c_0$  denotes the speed of sound (constant). Within the shell,  $\rho' = 0.5(r - c_0 t)\delta\rho/r$ ; where upon the gas is compressed in the outer portion of the shell  $r > c_0 t$  and rarefied in the inner portion  $r < c_0 t$ . Figure 1 shows the analytic and numerical NFT solution, the latter as specified below.

In the absence of a significant free-stream flow, the first term on the rhs of the equality in (6) reduces, virtually, to its linear kernel; that is, a centered-in-space (and time, as  $\mu \nearrow \infty$ ) approximation for (1). The resulting algorithm is dispersive [2], and the smooth solution in Figure 1 is achieved by enhancing dissipativity of the upwind advection with an  $\mathcal{O}(\delta x^2)$  residual, in the spirit of the FCT methods; see the Appendix in [11] and consider that our diffusion coefficient  $\nu = 0.02\delta x^2\delta t^{-1}$  is one order of magnitude smaller. To further substantiate the adequacy of MPDATA-based NFT schemes for wave propagation, we alter the classical problem as follows. An isothermal hemispherical density excess of  $\rho'/\rho_0 = 0.082$  with radius  $r_0 = 0.2$  m, is centered at the bottom of the  $6.38 \times 6.38 \times 3.19$  m<sup>3</sup> domain. A uniform free-stream flow is assumed with  $u_0 = c_0/3$ , where  $c_0 = 340.3$  m s<sup>-1</sup>. The domain is discretized with  $319 \times 319 \times 159$  uniform grid intervals  $\delta x = \delta y = \delta z = 0.02$  m; whereby,  $r_0 = 10\delta x$ . Numerical integrations of the posed initial value problem are carried out using constant temporal increment  $\delta t = 10^{-5}$  s. Boundary conditions are periodic in  $x$  and  $y$  and rigid in  $z$ .

Because the classical (linear) solution is Galilean invariant, the modified problem should yield the same solution as the classical problem in the reference frame translating with  $u_0$ . Indeed, the spherical wave propagates radially with  $c_0$ , away from the center translating with the free-stream flow. Figure 2 shows the NFT MPDATA solution after time  $t = 720\delta t$ . The selected time of the figure is long by the standards of, e.g. the Sod benchmark [12], purposely to emphasize the symmetry and phase errors; here  $c_0 t = 12.25 r_0 = 2.45$  m. In contrast to the result in Figure 1, the

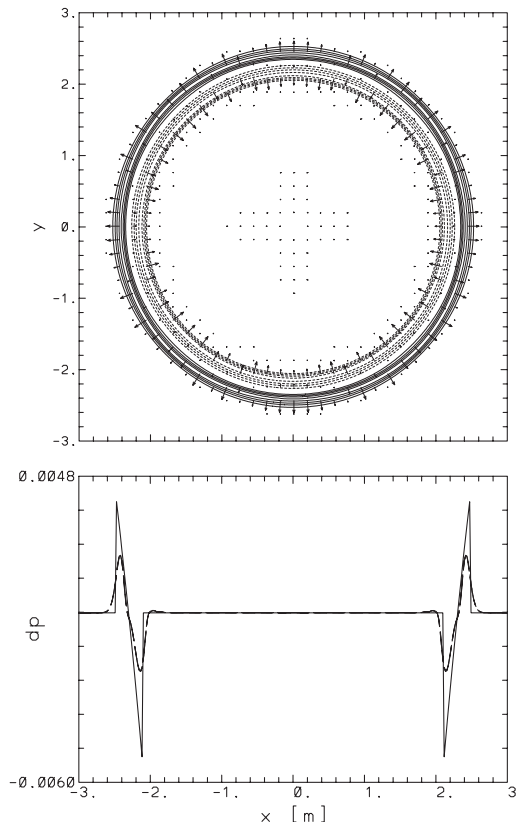


Figure 1. Spherical sound wave; normalized pressure perturbation  $\delta p = (p - p_0)/p_0$  at  $y = z = 0$  after  $t \gg r_0/c_0$  ( $r_0$  is the initial perturbation radius): (top) fully nonlinear 3D NFT result in the  $xy$  plane at  $z = 0$  with superimposed induced flow ( $\|\delta \mathbf{v}\|_\infty = 0.6 \text{ m s}^{-1}$ ); (bottom)  $\delta p$  at  $y = z = 0$  for the analytic solution (solid line) and the corresponding NFT result (dashed line).

solution in Figure 2 shows a slight symmetry breaking, presumably reflecting the Courant-number dependence of the truncation error characteristic of second-order advection schemes [13]. Here, we used basic MPDATA scheme with FCT monotonicity enhancement, and further improvements are possible [5, 6].

## 2.2. Aerodynamic benchmarks

The performance of the outlined algorithm is illustrated next for a steady-state transonic flow over an airfoil—AGARD test case 04 for NACA0012 airfoil at Mach number  $M = 0.8$  and incidence angle  $\alpha = 1.25^\circ$  [14], which we documented earlier [9] for the potential temperature equation in lieu of (5).

Figure 3 shows the standard display of the surface pressure coefficient  $C_p$  for the triangular and quadrilateral mesh, respectively. Identical numerics were used for both meshes. The MPDATA results show the sharp, single-point shock capturing that is consistent with the results discussed in [7, 9]. Additionally, the MPDATA solutions are compared with the Jameson Runge–Kutta

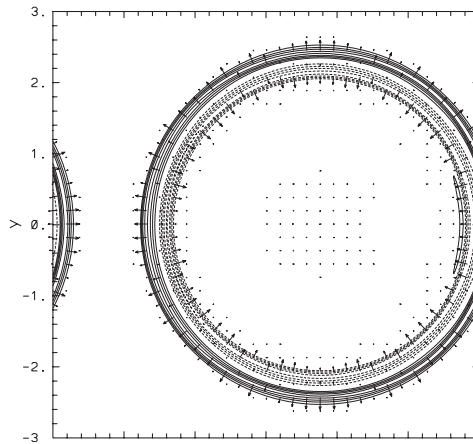


Figure 2. As in top panel of Figure 1 but in  $M = \frac{1}{3}$  free-stream flow, and with superimposed perturbation flow  $\delta\mathbf{v} = (u - u_0, v)$  vectors.

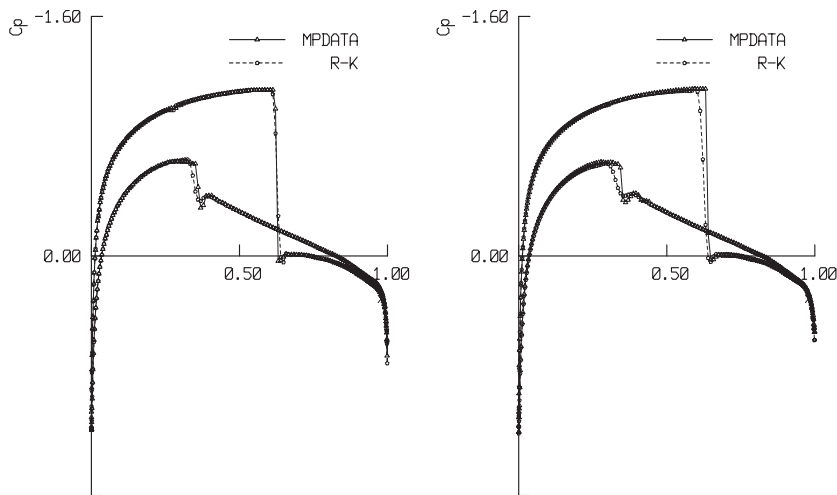


Figure 3.  $C_p$  pressure coefficient for NACA0012 airfoil;  $M = 0.8$ ,  $\alpha = 1.25^\circ$ . A comparison of MPDATA results with Runge–Kutta computations, for the triangular (left) and quadrilateral (right) meshes.

scheme [15]. Results from structured and unstructured meshes show that MPDATA gives a much sharper pressure jump on the weaker lower-surface shock (located in the region of higher wall curvature). Results for the structured mesh also indicate better upper shock capturing by MPDATA. MPDATA solutions use the FCT monotonicity enhancement [7] and relaxation of the antidiffusive correction in high gradient regions [9].

### 3. CONCLUSION

We introduced an NFT MPDATA solver for simulating gas dynamics, using a standard set of Euler equations important for high-speed flows. The results presented here, together with the earlier published evidence [9], demonstrate the validity of MPDATA for a range of fully compressible flows, from zero to high Mach number. Given the proficiency of the MPDATA-based NFT approach for studies in geophysics [8], the present development opens new avenues for simulation of environmental acoustics and extreme events.

### ACKNOWLEDGEMENTS

We would like to thank Professor Phillip L. Roe for his remarks on MPDATA that inspired this work.

### REFERENCES

1. Smolarkiewicz PK. On forward-in-time differencing for fluids. *Monthly Weather Review* 1991; **119**:2505–2510.
2. Smolarkiewicz PK, Margolin LG. On forward-in-time differencing for fluids: extension to a curvilinear framework. *Monthly Weather Review* 1993; **121**:1847–1859.
3. Smolarkiewicz PK, Dörnbrack A. Conservative integrals of adiabatic Durran's equations. *International Journal for Numerical Methods in Fluids* 2007; DOI: 10.1002/flid.1601.
4. Smolarkiewicz PK. A fully multidimensional positive definite advection transport algorithm with small implicit diffusion. *Journal of Computational Physics* 1984; **54**:325–362.
5. Smolarkiewicz PK, Margolin LG. MPDATA: a finite-difference solver for geophysical flows. *Journal of Computational Physics* 1998; **140**:459–480.
6. Smolarkiewicz PK. Multidimensional positive definite advection transport algorithm: an overview. *International Journal for Numerical Methods in Fluids* 2006; **50**:1123–1144.
7. Smolarkiewicz PK, Szmelter J. MPDATA: an edge-based unstructured-grid formulation. *Journal of Computational Physics* 2005; **206**:624–649.
8. Smolarkiewicz PK, Margolin LG. Studies in geophysics. In *Implicit Large Eddy Simulation: Computing Turbulent Fluid Dynamics*, Chapter 14, Grinstein FF, Margolin L, Rider W (eds). Cambridge Academic Press: Cambridge, 2007; 413–438.
9. Szmelter J, Smolarkiewicz PK. MPDATA error estimator for mesh adaptivity. *International Journal for Numerical Methods in Fluids* 2006; **50**:1269–1293.
10. Landau LD, Lifshitz EM. *Fluid Mechanics*. Elsevier: Amsterdam, 2004; 539.
11. Zalesak ST. A fully multidimensional flux-corrected transport algorithm for fluids. *Journal of Computational Physics* 1979; **31**:335–362.
12. Sod GA. A survey of several finite difference methods for systems of nonlinear hyperbolic conservation laws. *Journal of Computational Physics* 1978; **27**:1–31.
13. Margolin LG, Smolarkiewicz PK. Antidiffusive velocities for multipass donor cell advection. *SIAM Journal on Scientific Computing* 1998; **20**(3):907–929.
14. AGARD. Test cases for inviscid flow field methods. *AGARD Advisory Report No. 211*, AGARD-AR-211, 1985.
15. Jameson A, Schmidt W, Turkel E. Numerical solution of the Euler equations by finite volume methods using Runge–Kutta time-stepping schemes. *AIAA 81-1259 Paper*.